Synthesis and structure of hydroxyapatite/tannin composites

Lia Anggresani[1), 2)] (ORCID ID: 0000-0002-4491-8484), **Aster Rahayu**[3), *)] (0000-0003-4995-5249), **Santi Perawati**[4)] (0000-0002-7357-748X), **Yulianis Yulianis**[5)] (0000-0002-3271-8979), **Ulma Sintia**[5)], **Randi Setiawan**[5)]

DOI: https://doi.org/10.14314/polimery.2024.9.2

Abstract: Hydroxyapatite (HA)-tannin composites were obtained by precipitation using $Ca(OH)_2$ as calcium precursor and $(NH_4)_2HPO_4$ or H_3PO_4 as phosphate precursors, with tannin acting as a chelating agent. FT-IR confirmed the presence of functional groups derived from tannin in the composite, and XRD showed trace amounts of calcium carbonate. The crystal sizes of HA and HA/tannin were 15–27 nm and 10–29 nm, respectively. SEM showed agglomeration of HA and HA/tannin particles. The size distribution of HA particles was in the range of 0.1–0.2 μm (without tannin), and the size distribution of HA/tannin particles in the range of 0.1–0.4 μm. The obtained results confirmed the formation of strong bonds between tannin and HA.

Keywords: chelating agent, diammonium hydrogen phosphate, phosphoric acid, tannin.

Synteza i struktura kompozytów hydroksyapatyt/tanina

Streszczenie: Metodą wytrącania otrzymano kompozyty hydroksyapatytu (HA) z taniną, stosując $Ca(OH)_2$ jako prekursor wapnia i $(NH_4)_2HPO_4$ lub H_3PO_4 jako prekursory fosforanu, przy czym tanina pełniła rolę środka chelatującego. Analiza FT-IR potwierdziła obecność w kompozycie grup funkcyjnych pochodzących z taniny, a analiza XRD wykazała śladowe ilości węglanu wapnia. Wielkość kryształów HA i HA/tanina wynosiła odpowiednio 15–27 nm i 10–29 nm. SEM wykazało aglomerację cząstek HA i HA/tanina. Rozkład wielkości cząstek HA mieścił się w przedziale 0,1–0,2 μm (bez taniny), a rozrzut wielkości cząstek HA/tanina w przedziale 0,1–0,4 μm. Uzyskane wyniki potwierdziły tworzenie się silnych wiązań między taniną a HA.

Słowa kluczowe: środek chelatujący, wodorofosforan diamonu, kwas fosforowy, tanina.

Hydroxyapatite (HA) is widely used in healthcare, especially in bone and tooth repair, as well as wound healing. HA plays a significant role in the development of biomedical and biomaterial sciences [1, 2]. The progress in the synthesis of biomaterials for bone and dental tissue aims to enhance cell growth, which in turn supports the functional life cycle in the case of tissue replacement [3]. One of the advantages of HA is its stability and durability as an implant material [4]. Currently, hydroxyapatite is used as a tissue additive or substitute. It is an inorganic biomaterial, a calcium phosphate compound, with a structure like human bones and teeth [5]. HA can be synthesized from inorganic materials such as phosphate solutions [6]. However, the chemicals used in this process have a negative impact on the environment, and the production costs are high [7, 8].

Hydroxyapatite ($Ca_{10}(PO_4)_6(OH)_2$) is the main mineral component of bone, consisting of calcium phosphate compounds. It is widely used as a biomaterial due to its biocompatibility, which supports cellular functions, and osteoconductive properties, which are key features of bioceramics [9]. Hydroxyapatite can be synthesized by mixing calcium and phosphate in a molar ratio of 1.67 [10]. It can be produced from natural or chemical sources. Studies have been conducted on the synthesis of hydroxyapatite from natural materials such as eggshells, crab shells, mackerel bones, beef bones, and limestone from Bukit Tui in Padang Panjang, Indonesia [11–13].

Currently, the main application of synthetic hydroxyapatite is in contact with bone tissue and as a biocompatible

[1)] Material Engineering Division, Faculty of Engineering, Gifu University, 1-1 Yanagido, Gifu, 501-1193, Japan.

[2)] Department of Midwifery, Syedza Saintika University, Padang, Sumatera Barat 25132, Indonesia.

[3)] Department of Chemical Engineering, Faculty of Industrial Technology, Universitas Ahmad Dahlan, Yogyakarta 55166, Indonesia.

[4)] Department of Pharmacy, Faculty of Medicine and Health Science, Jambi University, Jambi City 36361, Indonesia.

[5)] Department of Pharmacy, College School of Health Science Harapan Ibu Jambi, Jambi 36122, Indonesia.

[*)] Author for correspondence: aster.rahayu@che.uad.ac.id

ceramic coating for bone implants in the human body [14, 15]. HA can be prepared by various methods, such as hydrothermal or microwave synthesis, co-precipitation, freezing, and ultrasonic irradiation [16, 17]. HA is most obtained by the precipitation method, due to its simplicity and availability of raw materials [18]. Different synthesis processes allow the production of HA with different particle sizes, shapes, and homogeneity [16, 19]. The precipitation method is performed by controlling the solubility of the material in the solution by changing the pH, temperature, or solvent.

Biopolymers are defined as polymers produced from biological sources, obtained from microorganisms, algae, or plants [20]. Cellulose and starch are considered the simplest biopolymers and are widely developed in the fields of medicine and food production. Biopolymers can be synthesized by chemical and physical methods, depending on the type of polymer. Animals can produce collagen, which is one of the structural proteins found in many hard tissues, especially bones (38%) and is a mediator of osteoblast cells [21]. Collagen is widely used as a biomaterial due to its biodegradable properties, biocompatibility, ability to form scaffolds and pores, and accelerates the bone healing process [22]. For the above reasons, collagen is used as bone implants. Hydroxyapatite has excellent biocompatibility, immunogenicity and is non-toxic to the human body [23]. Despite many advantages, HA has poor mechanical properties. To obtain a composite with excellent mechanical properties, polymers are used in the production process. Hydroxyapatite nanotubes were synthesized using Moringa oleifera flower extract by microwave-assisted method [18]. Meanwhile, Sundararajan *et al*. [24] described the synthesis of hydroxyapatite nanoplatelets using Moringa oleifera flower extract. In both works, tannin from Moringa oleifera flower extract was used as a polymer. These tannins have molecular formula $C_{76}H_{52}O_{46}$ and are polyphenolic compounds that have chelating properties due to phenolic and hydroxyl groups in their structure [24]. The study [25] presents a method for the synthesis of HA using a novel ultrasonic excipient, showing that increasing the ultrasonic irradiation time reduces both the crystallinity and the size of HA nanoparticles. The synthesis of hydroxyapatite using tannins as a chelating agent is an interesting research topic in the field of biomaterials and biomedicine. Tannins, as natural polyphenolic compounds, can be extracted from various plants and can bind with phosphate ions in solutions to help control the formation and size of hydroxyapatite crystals [26]. Tannins concentration, reagents ratio, solution pH, temperature and reaction time affect the physicochemical properties and structure of HA.

Therefore, in this work, the use of tannin as chelating agent for the synthesis of hydroxyapatite by precipitation was studied. HA was synthesized from $Ca(OH)_2$, and phosphoric precursors such as H_3PO_4 and diammonium hydrogen phosphate $(NH_4)_2HPO_4$. FT-IR, XRD and SEM were used to characterize HA. The hardness was also determined.

EXPERIMENTAL PART

Materials

Tannic acid ($C_{76}H_{52}O_{46}$, molecular weight – 1701.20 g/mol), calcium hydroxide [$Ca(OH)_2$, molecular weight – 74.09 g/mol], diammonium hydrogen phosphate [$(NH_4)_2HPO_4$, molecular weight – 132.06 g/mol], phosphoric acid 85% (H_3PO_4, density – 1.71 g/mL), sodium hydroxide (NaOH, molecular weight – 40 g/mol) and deionized water were purchased from Merck (Darmstadt, Germany).

Synthesis of hydroxyapatite

The hydroxyapatites were prepared using two precursors, H_3PO_4 and $(NH_4)_2HPO_4$ with and without tannins. A 250 mL of 1 M $Ca(OH)_2$ was stirred for 10 min using a magnetic stirrer. Then, a 250 mL of 0.6 M precursor solution was added with 0.8 M NaOH to achieve 12 pH. Then, the stirring continued for 1 h. The samples were then left for 24 h at room temperature. After this time, the hydroxyapatite obtained was filtered using filter paper. The residue was dried in an oven at 400°C (with tannin) and 800°C (without tannin) for 5 h. The dried residue was weighed and characterized using appropriate methods.

Methods

Basic organoleptic analysis was performed, and the color and odor of hydroxyapatite were assessed.

Fourier infrared spectroscopy (FT-IR) (Perkin Elmer, model Spotlights 400, Waltham, MA, US) was used to analyze the chemical structure. The spectra were recorded using at least 50 scans with 2 cm^{-1} resolution, in the spectral range of 4000–400 cm^{-1}, using KBr pellets technique. X-ray diffraction (XRD) measurements were performed on Panalytical X'PERT Pro (Phillips) diffractometer (The Netherlands) using CuKα radiation (λ = 1.54 Å) with 40 kV and 30 mA. The structure was determined using a Hitachi TM3000® (Tokyo, Japan) scanning electron microscope (SEM). Other equipment used in this study included an analytical balance (Ohaus® USA), magnetic stirrers (IKA® C-MAG HS7) Japan, a furnace (Binder®) India, an electric tablet press Maksindo type MKS-TBL-55, tablet hardness tester model EH-01P (Electrolab, USA) with hardness range up to 500 N, and an L-301 XSZ-107BN ocular microscope.

RESULTS AND DISCUSSION

Organoleptic analysis

In this study, two different synthesis methods were used, namely the synthesis of pure hydroxyapatite (HA) and hydroxyapatite with added tannin (HA/tannin).

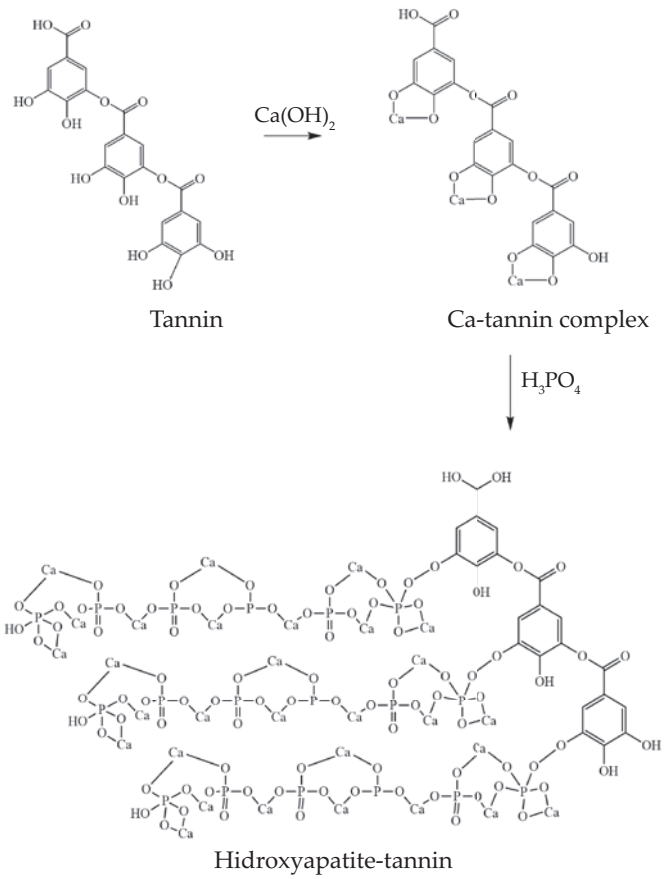

Fig. 1. Hydroxyapatite/tannin structure using H_3PO_4 precursor

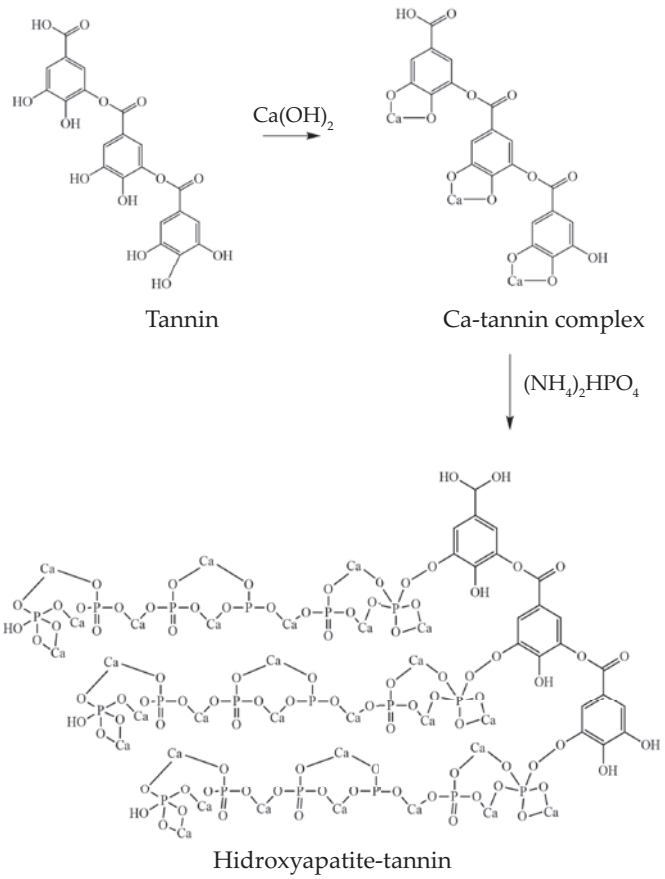

Fig. 2. Hydroxyapatite/tannin structure using $(NH_4)_2HPO_4$ precursor

The results showed differences in color and odor. Pure hydroxyapatite is white, while hydroxyapatite with tannins is brownish white. This color difference is caused by the interaction between hydroxyapatite and tannins, which leads to the formation of new compounds or a change in the crystal structure of hydroxyapatite. The white color indicates purity and cleanliness, while the brown color may indicate the presence of impurities or additional chemical reactions. Pure hydroxyapatite has no significant odor, whereas HA/tannin has a slightly pungent odor. The odor that appears in hydroxyapatite with added tannins is due to the chemical nature of the tannins themselves or a chemical reaction between the tannins and the hydroxyapatite components. Tannins naturally have a strong, characteristic aroma. Adding tannins to hydroxyapatite can affect its odor.

FT-IR analysis

FT-IR analysis was performed to identify the functional groups of HA/tannin including OH, PO_4^{3-}, C-H, C=C and CO_3^{2-} in the range of 4000–400 cm^{-1} [27]. The samples were ground into powder to facilitate FT-IR analysis. Figures 1 and 2 show HA/tannin structure obtained using different precursors, and Figures 3 and 4 the FT-IR spectra. FT-IR can provide valuable information about the chemical characteristics of HA, including composition, purity, presence of impurities, and interactions with tannin additives.

The FT-IR spectrum of HA displays the characteristic peak related to phosphate bond vibrations (500–600 cm^{-1}), phosphate and carbonate bonds (1000–1100 cm^{-1}), hydroxyl (OH-) groups (1600–1700 cm^{-1}), and free or bound hydroxyl (OH-) groups (3400–3600 cm^{-1}) [27]. The presence of carbonate in HA may affect its physicochemical properties and biocompatibility. The absorption of hydroxyl groups can provide information about the purity and stability of HA. In contrast, HA/tannin spectra show a displacement in several peaks. The peak at 3361 cm^{-1} shifted to 3225 cm^{-1}, 1643 cm^{-1} to 1647 cm^{-1}, 1421 cm^{-1} to 1424 cm^{-1}, and 1026 cm^{-1} to 1016 cm^{-1}. The carbonyl groups (C=O) in tannin were difficult to distinguish due to their involvement in strong interactions or complexation with HA and it overlapped with other peaks in the spectrum. This causes the carbonyl peak to shift or become less prominent.

The presence of OH^- and $PO4^{3-}$ functional groups in HA/tannin spectra (Figs. 3b and 4b) indicated the formation of hydroxyapatite [28]. Based on Sigma-Aldrich literature on IR spectrum analysis, the C-H functional group with vibrational bending occurs in the wavenumber range of 2000–1650 cm^{-1}. The peaks, related to C=C stretching vibrations, are located at wavenumbers 1647 cm^{-1}, 1644 cm^{-1}, and 1643 cm^{-1}, it is an aromatic ring group in the range of 1670–1620 cm^{-1} [27].

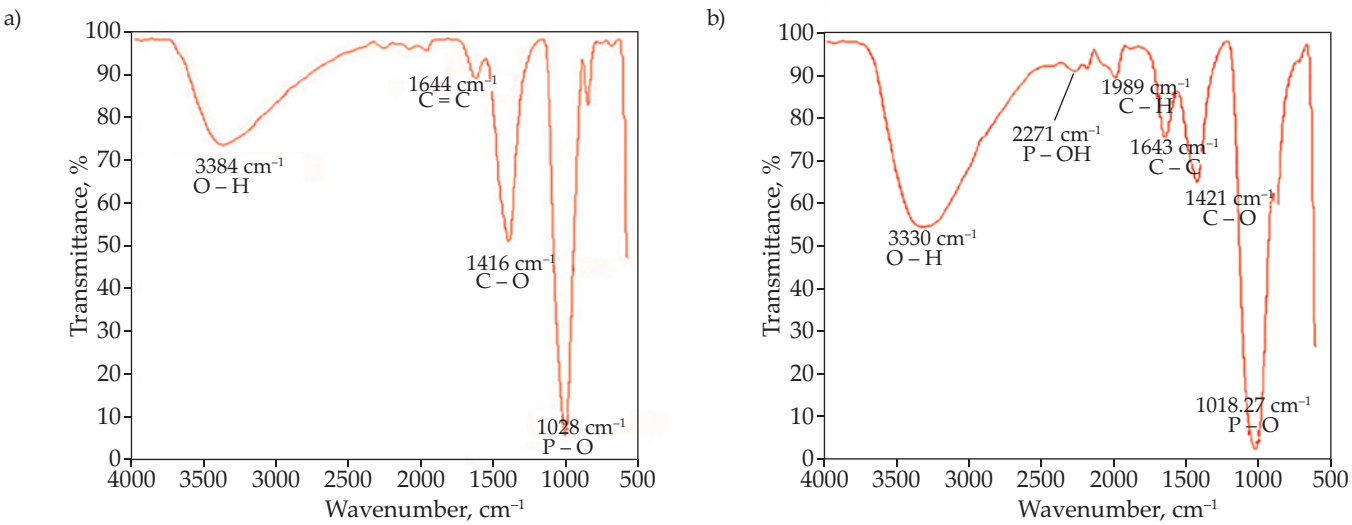

Fig. 3. FT-IR spectra of HA with H_3PO_4 as a precursor: a) pure HA, b) HA/tannin

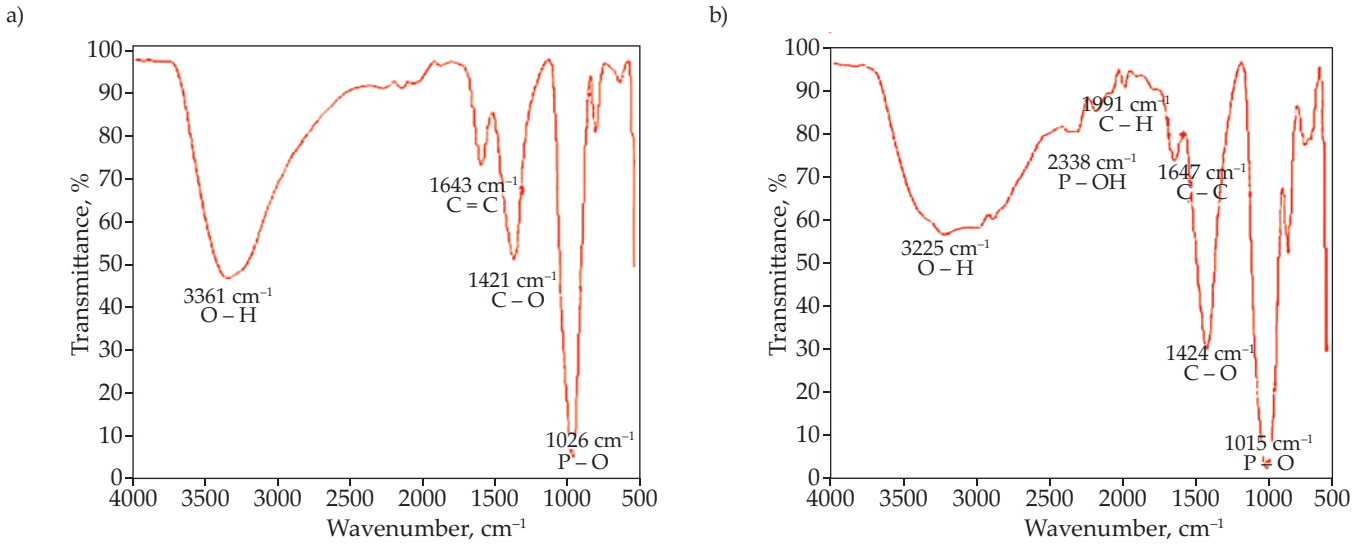

Fig. 4. FT-IR spectra of HA with $(NH_4)_2HPO_4$ as a precursor: a) pure HA, b) HA/tannin

The change in bond energy causes a shift in the wavenumber, the increase in energy, and a stronger bond between HA and species, particularly tannin. In addition, the presence of functional groups O-H, C=C aromatic and C-H, which indicate the functional groups of tannin compounds, confirms that tannin functioned as chelating agent due to phenolic effects (Fig. 1 and Fig. 3).

Furthermore, tannins can form strong bonds with HAs, which confirm bond changes and the presence of functional groups corresponding to tannin compounds.

This finding has important implications for the application of tannin as a chelating agent or other related materials because it can improve the physicochemical properties and performance of the material. Several previous studies have revealed relevant results regarding peak shifts in FT-IR spectra and the role of tannins as chelating agents. Research conducted by [29] shows that HA has two peaks at 3225 and 3058 cm^{-1} associated with the presence of hydroxyl (OH^-). Research from [17] also reported a shift in the FT-IR spectra at wavenumber 3570 cm^{-1} associated with the presence of hydroxyl (OH^-). Phosphate bands were appreciated at 1092 to 1040 cm^{-1}, 962 cm^{-1}, 633–566 cm^{-1} and 473 cm^{-1}, respectively.

XRD analysis

XRD analysis was performed to determine the crystal structure and size of crystals. The analysis revealed the formation of two compounds: calcium carbonate and hydroxyapatite. The results were compared to 20 positions in the diffractogram with data from the Inorganic Crystal Structure Database (ICSD). ICSD No. 01-072-1243 confirmed the presence of hydroxyapatite, while ICSD Nos. 01-085-1108 and 01-078-3262 indicated the presence of calcium carbonate.

The samples, compared with the standard Hydroxyapatite-Tannin Inorganic Crystal Structure Database (ICSD) entries No. 01-074-0566 and No. 01-072-1243, indicate the presence of hydroxyapatite. ICSD entries No. 01-075-6049 and No. 01-083-1762 confirm the presence of calcium carbonate. The peaks in the diffractogram revealed more calcium carbonate compounds than hydroxyapatite, as shown in Figs 5

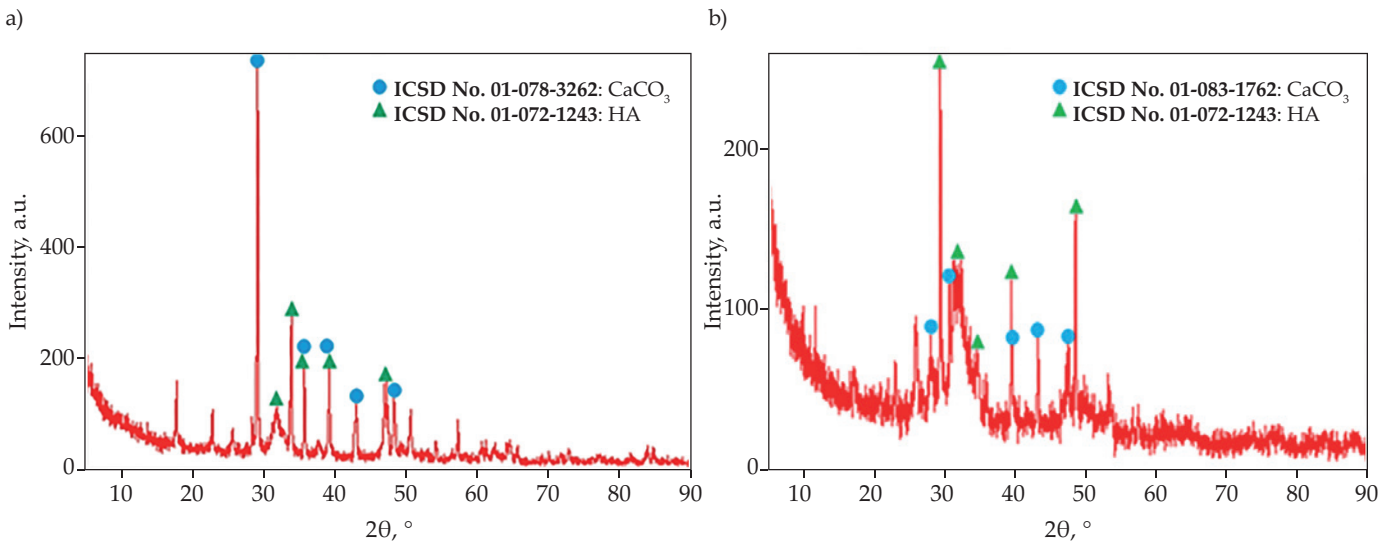

Fig. 5. XRD patterns of HA with H_3PO_4 as a precursor: a) pure HA, b) HA/tannin

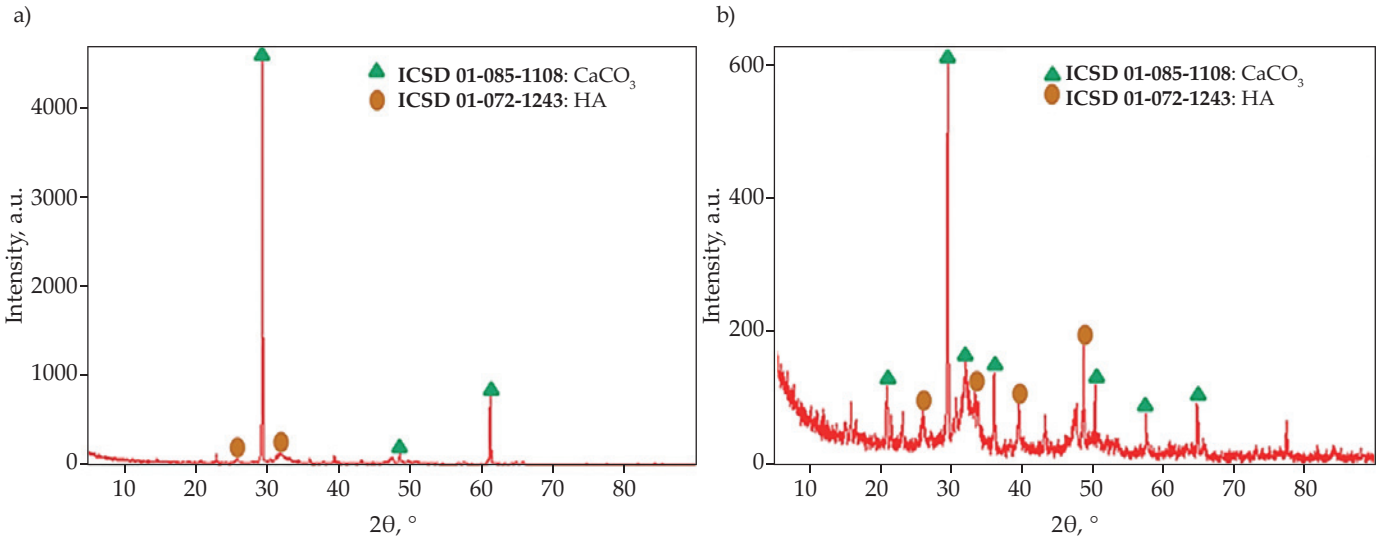

Fig. 6. XRD patterns of HA with $(NH_4)_2HPO_4$ as a precursor: a) pure HA, b) HA/tannin

and 6. These findings have significant implications for understanding the composition and structure of HA and HA/tannin. The presence of calcium carbonate in hydroxyapatite samples may influence the physical and chemical properties of the material.

The purity of the produced hydroxyapatite is not yet optimal due to the presence of $CaCO_3$. Carbonate groups (CO_3^{2-}) originate from the reaction of hydroxyapatite with carbon dioxide (CO_2) present in the atmosphere during synthesis and heat treatment. The carbonate ions formed can enter the crystal lattice of hydroxyapatite, replacing hydroxyl ions (OH^-) or phosphate ions, which affect the crystal structure and change the Ca/P molar ratio. The presence of carbonate ions is not necessarily undesirable, as human bones naturally contain carbonate ions that replace phosphate in the form of carbonated hydroxyapatite (CHA), following the equation $Ca_{10}(CO_3)_x(PO_4)_{6-}(2/3)_x(OH)_2$.

X-ray diffraction patterns can also provide information about crystal size. It can be determined using the Scherrer method, where a sharp peak with a narrow width indicates a large crystal size, while a broadened peak suggests a smaller crystal size. The crystal size is calculated by measuring the full width at half maximum (FWHM) of the peak with the highest intensity. For the hydroxyapatite crystals derived from the H_3PO_4 precursor, the sizes ranged from 15.5 to 20.8 nm, while for hydroxyapatite with added tannin, the range was 15.4 to 21.8 nm. In comparison, hydroxyapatite crystals from the diammonium hydrogen phosphate precursor measured between 15 and 27 nm, and with the addition of tannin, the range was 10 to 29 nm. The difference between morphological measurements and the calculations using the Scherrer method can be attributed to several factors, including the overestimation of particle size in morphological measurements (where the longest axis of the particle is measured) and the subjective nature of morphological measurement (where only a few particles are measured, making it less representative). Hydroxyapatite with the addition of tannin as a chelating agent shows a wide size range, indicating the formation of larger crystals.

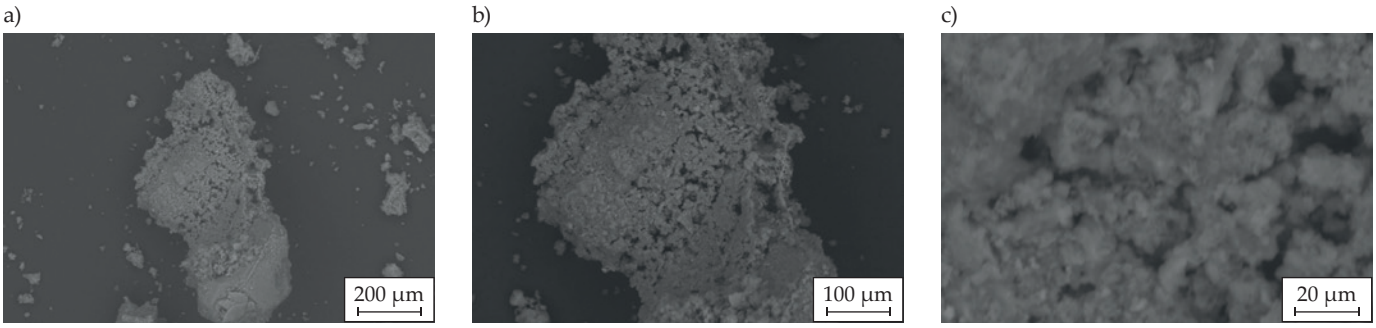

Fig. 7. SEM images of HA with H_3PO_4 as a precursor at different magnification: a) 500×, b) 1000×, c) 5000×

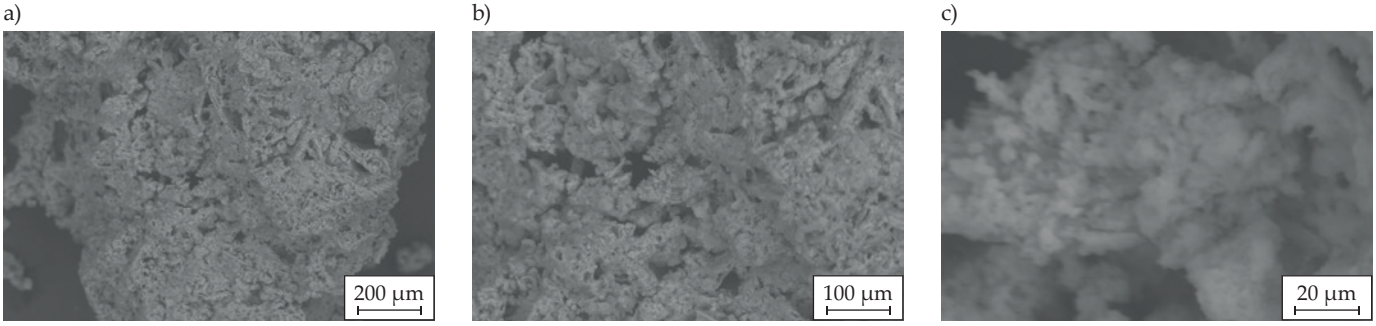

Fig. 8. SEM images of HA/tannin with H_3PO_4 as a precursor: a) 500×, b) 1000×, c) 5000×

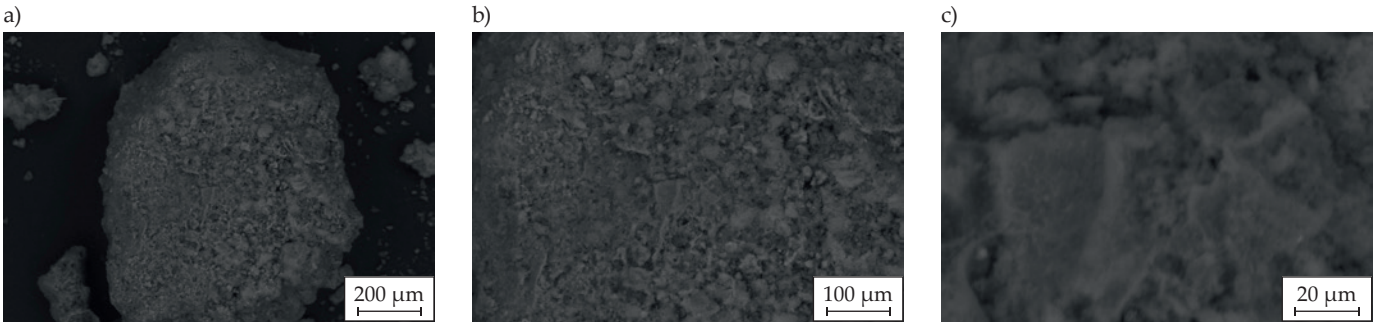

Fig. 9. SEM images of HA with $(NH_4)_2HPO_4$ as a precursor: a) 500×, b) 1000×, c) 5000×

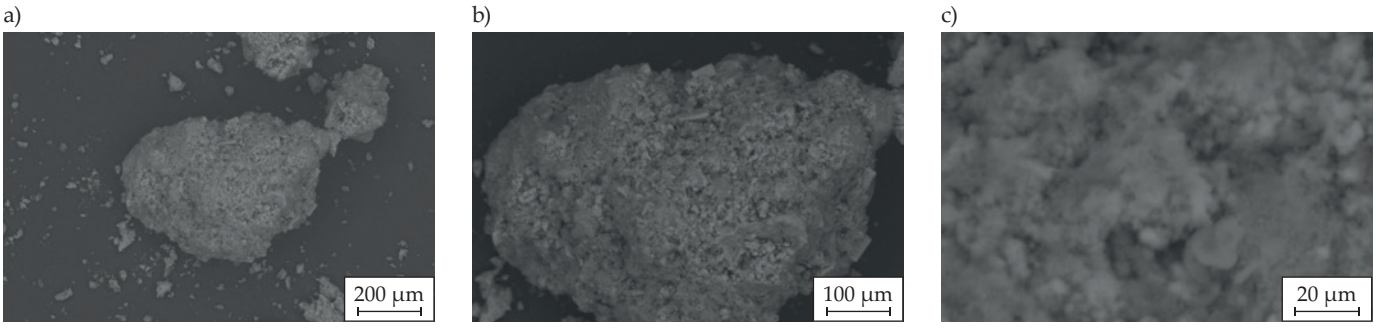

Fig. 10. SEM images of HA/tannin with $(NH_4)_2HPO_4$ as a precursor: a) 500×, b) 1000×, c) 5000×

SEM analysis

SEM analysis was performed to observe the surface structure of the formed hydroxyapatite particles. From Figs. 7–10 t can be observed that HA particles were agglomerated or stuck together, due to the inhomogeneity during synthesis, which caused them to stick together during the heating process. The particle size distribution of HA varies from 0.1–0.2 μm (without tannin), while the particle size of HA/tannin varies from 0.1–0.4 μm. Smaller hydroxyapatite particle size results in a larger specific surface area, which is associated with stronger interactions between hydroxyapatite and tannins [9]. The particle size of HA can be increased by adding tannins, which may be significant for HA applications. Due to the larger surface area, HA has a better potential for interaction with the surrounding environment and various substances or molecules, including tannins. This may affect

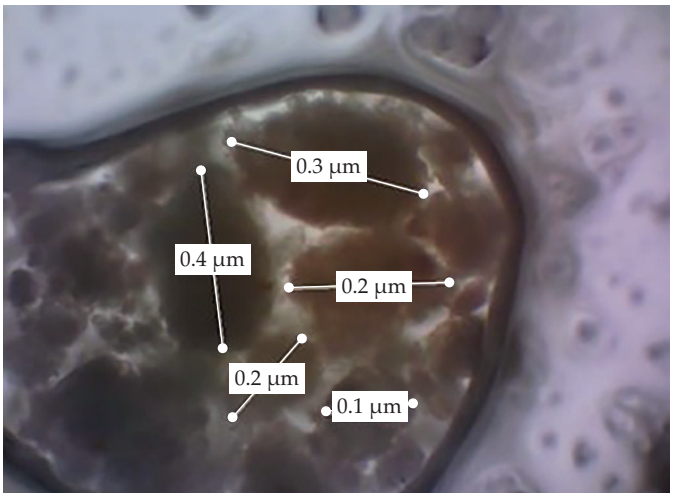

Fig. 11. Particle size of HA/tannin (precursor H_3PO_4)

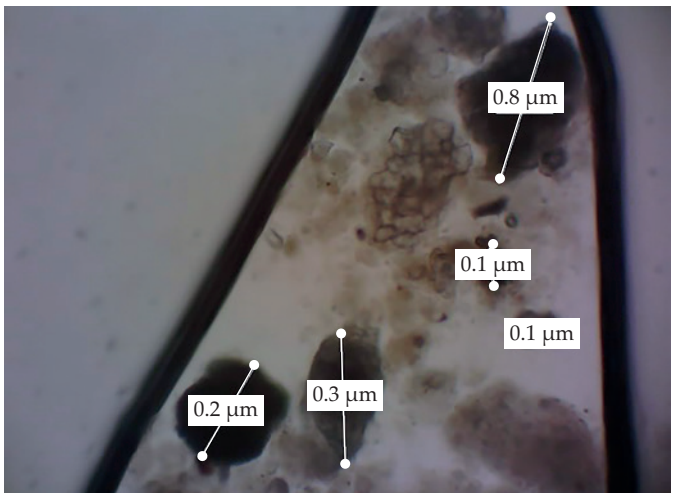

Fig. 12. Particle size of HA/tannin [precursor $(NH_4)_2HPO_4$]

the physicochemical properties of hydroxyapatite and the interactions of HA with other chemical species. The bond between HA and tannin can also have an impact on the stability of HA/tannin in the studied system. A stronger bond can strengthen the interaction between two components, which affect the physical and chemical stability of HA/tannin. However, it is important to remember that this analysis only allows for assessment of particle size and the bond between HA and tannin. In the context of HA/tannin applications, further research is needed to evaluate the effects of particle size and bonding on material properties, such as stability, biocompatibility, and drug delivery ability.

The results of previous studies can also provide relevant comparisons related to the particle size distribution of hydroxyapatite and the effect of tannins. It was observed that hydroxyapatite without the addition of tannins has a more homogeneous particle size distribution [30]. This shows that the addition of tannins can affect the particle size distribution of hydroxyapatite. In addition, tannins have a strong affinity for the hydroxyapatite surface and form stable bonds [31].

Hardness

The hydroxyapatite powder was pressed into tablets, which were then analyzed for hardness. The average hardness of HA was about 28 N and HA/tannin about 34 N, which may indicate the higher compressive strength of HA/tannin, as shown in Figures 11 and 12.

Hardness is a commonly used method to measure a material's resistance to plastic deformation or penetration. The hardness provides insights into the material's strength and resistance to compressive loads. In this study, the results demonstrated that hydroxyapatite with the addition of tannins had higher hardness than hydroxyapatite without tannins. This suggests that the addition of tannins as a chelating agent increased the compressive strength of hydroxyapatite. The improvement in compressive strength could be attributed to several factors. First, tannins may form strong bonds with hydroxyapatite, enhancing structural stability and reducing deformation. Additionally, interactions between tannins and hydroxyapatite can result in the formation of hydrogen bonds and strong dispersion forces, which increase the intermolecular forces within the material.

CONCLUSIONS

Hydroxyapatite was successfully synthesized using $Ca(OH)_2$ as calcium precursor and $(NH_4)_2HPO_4$ or H_3PO_4 as phosphate precursors by precipitation method, with tannin acting as chelating agent. The results showed that pure hydroxyapatite is white, odorless, and tasteless. However, hydroxyapatite with the addition of tannin showed brownish-white color and slightly pungent odor. FT-IR indicated the presence of functional groups derived from tannin in the modified hydroxyapatite. X-ray diffraction showed that hydroxyapatite contained traces of calcium carbonate. SEM showed agglomeration of hydroxyapatite particles. It was confirmed that tannins can form strong bonds with hydroxyapatite. The results obtained may contribute to the development of hydroxyapatite applications in medicine or in the food field.

ACKNOWLEDGEMENTS

The authors are grateful to the Directorate of Simbelmawa Republic of Indonesia for the Student Creativity Program Grant 2020.

Authors contribution

L.A – conceptualization, methodology, validation, resources, data curation, writing-review and editing, visualization, supervision, funding acquisition; A.R. – validation, data curation, writing-review nd editing, visualization; S.P. – conceptualization, methodology, validation, resources, writing-review and editing, supervision, funding acquisition; Y.Y. – validation, writing-review and editing, supervision, project administration; U.S. – writing-original draft, methodology, formal analysis, investigation; R.S. – writing-original draft, methodology, formal analysis, investigation.

Funding
The authors are grateful to the Directorate of Simbelmawa Republic of Indonesia for the Student Creativity Program Grant 2020.

Conflict of interest
The authors have stated no conflict of interest. There is no potential for plagiarism in data collection or preparation of papers.

REFERENCES

[1] Hussin M.S.F., Abdullah H.Z., Idris M.I. *et al*.: *Heliyon* **2022**, *8*, e10356. https://doi.org/10.1016/j.heliyon.2022.e10356
[2] Siddiqui H.A., Pickering K.L.: *Materials* **2018**, *11(10)*, 1813. https://doi.org/10.3390/ma11101813
[3] E. Andronescu, Grumezescu A.M., Guşă M.I. *et al.*: "Nano-hydroxyapatite: Novel approaches in biomedical applications" (edit. Grumezescu A.M.), William Andrew Publishing, 2016, p. 189. https://doi.org/10.1016/B978-0-323-42862-0.00006-7
[4] Saini M., Singh Y., Arora P. *et al*.: *World Journal of Clinical Cases* **2015**, *3(1)*, 52. https://doi.org/10.12998/wjcc.v3.i1.52
[5] Ragu A., Sakthivel P., Senthilarasan K.: *International Journal of Science and Research* **2015**, *4*, 1220.
[6] Mohd Pu'ad N.A.S., Koshy P., Abdullah H.Z. *et al*.: *Heliyon* **2019**, *5(5)*, e01588. https://doi.org/10.1016/j.heliyon.2019.e01588
[7] Arokiasamy P., Al Bakri Abdullah M.M., Abd Rahim S.Z. *et al.: Ceramics International* **2022**, *48(11)*, 14959. https://doi.org/10.1016/j.ceramint.2022.03.064
[8] Fiume E., Magnaterra G., Rahdar A. *et al*.: *Ceramics* **2021**, *4(4)*, 542. https://doi.org/10.3390/ceramics4040039
[9] Pramanik N., Mishra D., Banerjee I. et al.: *International Journal of Biomaterials* 2009, 1, 512417. https://doi.org/10.1155/2009/512417
[10] Manoj M., Subbiah R., Mangalaraj D. *et al*.: *Nanobiomedicine* **2015**, *2*. https://doi.org/10.5772/60116
[11] Supangat D, Cahyaningrum S.E.: *UNESA Journal of Chemistry* **2017**, *6(3)*, 143.
[12] Varadavenkatesan T., Vinayagam R., Pai S. *et al*.: *Progress in Organic Coatings* **2021**, *151*, 106056. https://doi.org/10.1016/j.porgcoat.2020.106056
[13] Shi P., Liu M., Fan F. *et al*.: *Materials Science and Engineering: C* **2018**, *90*, 706. https://doi.org/10.1016/j.msec.2018.04.026
[14] Suchanek W., Yoshimura M.: *Journal of Materials Research* **1998**, *13(1)*, 94. https://doi.org/10.1557/JMR.1998.0015
[15] Swetha M., Sahithi K, Moorthi A. *et al*.: *International Journal of Biological Macromolecules* **2010**, *41(1)*, 1. https://doi.org/10.1016/j.ijbiomac.2010.03.015
[16] Lala S.D., Deb P., Barua E. et al.: *Materials Today: Proceedings* 2019, 15(2), 323. https://doi.org/10.1016/j.matpr.2019.05.012
[17] Khurshid Z., Alfarhan M.F., Mazher J. *et al.: Molecules* **2022**, *27(22)*, 7946. https://doi.org/10.3390/molecules27227946
[18] Kalaiselvi V., Mathammal R., Vijayakumar S. *et al*.: *International Journal of Veterinary Science and Medicine* **2018**, *6(2)*, 286. https://doi.org/10.1016/j.ijvsm.2018.08.003
[19] Yenti S.R., Faldi A., Wisrayetti W. *et al.: Materials Today: Proceedings* 2023, 87(2), 278. https://doi.org/10.1016/j.matpr.2023.03.282
[20] A. Meraldo: "Introduction to Bio-Based Polymers" in "Multilayer Flexible Packaging" (edit. Wagner Jr. J.R.), William Andrew Publishing 2016, p. 47. https://doi.org/10.1016/B978-0-323-37100-1.00004-1
[21] Chen X., Wang Z., Duan N. *et al*.: *Connective Tissue Research* **2018**, *59*, 99. https://doi.org/10.1080/03008207.2017.1290085
[22] Chen Q., Bruyneel A., Clarke K. *et al*.: *Journal of Tissue Science & Engineering* **2012**, *S11*, 1. https://doi.org/10.4172/2157-7552.S11-003
[23] Ramesh S., Loo Z.Z., Tan C.Y. *et al.: Ceramics International* **2018**, *44(9)*, 10525. https://doi.org/10.1016/j.ceramint.2018.03.072
[24] Sundararajan M., Jegatheeswaran S., Selvam S. *et al*.: *Materials and Design* **2015**, *88*, 1183.
[25] Gopi D., Indira J., Kavitha L. *et al*.: *Spectrochimica Acta Part A: Molecular and Biomolecular Spectroscopy* 2012, 93, 131. https://doi.org/10.1016/j.saa.2012.02.033
[26] Alorku K., Manoj M., Yuan A.: *RSC Advances* **2020**, *10*, 40923. https://doi.org/10.1039/d0ra08529d
[27] Nandiyanto A.B.D., Oktiani, Ragadhita R.: *Indonesian Journal of Science and Technology* **2019**, *4(1)*, 97.
[28] Supriyono S., Kartikowati C.W., Poerwadi B. *et al.: International Journal of Technology* **2023**, *14(2)*, 330. https://doi.org/10.14716/ijtech.v14i2.4452
[29] Yang Y, Abdalla S.: *Frontiers in Bioengineering and Biotechnology* 2020, 8, 951. https://doi.org/10.3389/fbioe.2020.00951
[30] Vázquez M.S., Estevez O., Acencio-Aguirre F. *et al*.: *Applied Physics A* **2016**, *112*, 868. https://doi.org/10.1007/s00339-016-0363-6
[31] Velmurugan P, Ramaprasad E.R.A., Jonnalagadda R.P. *et al*.: *Biopolymers* **2013**, *101(5)*, 471. https://doi.org/10.1002/bip.22405

Received 25 VII 2024.
Accepted 15 VIII 2024.